PCCP

Non-oxidative reactions of propane on Zn/Na-ZSM5

Joseph A. Biscardi and Enrique Iglesia*

Department of Chemical Engineering, University of California, Berkeley, California 94720, USA. E-mail: iglesia@cchem.berkeley.edu; Fax: + 1510 642 4778

Received 11th August 1999, Accepted 12th October 1999

Propene formation rates during propane conversion at 773 K on Zn/Na-ZSM5 are about ten times higher than on Zn/H-ZSM5 catalysts with similar Zn content. The total rate of propane conversion is also higher on Zn/Na-ZSM5 by a factor of four. Propane reactions lead to high propene selectivities (>50%) as protons are replaced by Na cations in Zn/H-ZSM5 catalysts. The titration of acid sites with Na^+ cations decreases the rate of acid-catalyzed chain growth reactions and the selectivity to C_6–C_9 aromatics. X-ray absorption studies at the Zn-K edge showed that aqueous ion exchange of Na-ZSM5 with Zn cations leads to isolated $(ZnOH)^+$ species located at cation exchange sites. Unlike Zn species in Zn/H-ZSM5 (<1.0 wt.%), high temperature condensation reactions of $(ZnOH)^+$ species with neighboring zeolite OH groups are less likely to occur in Zn/Na-ZSM5 and most Zn species remain as $(ZnOH)^+$. Temperature programmed reduction studies show that Zn species in Zn/Na-ZSM5 reduce at lower temperatures than the $(O^-–Zn^{2+}–O^-)$ species present in Zn/H-ZSM5. D_2 exchange with surface OH groups showed that some protons are formed during ion exchange. Higher deuterium contents in products of C_3H_8–D_2 mixtures on Zn/Na-ZSM5 suggest that $(ZnOH)^+$ species in Zn/Na-ZSM5 catalyze rate-determining hydrogen desorption steps during propane conversion more effectively than $(O^-–Zn^{2+}–O^-)$ sites present in Zn/H-ZSM5. The presence of $(ZnOH)^+$ species and a lower acid site density in Zn/Na-ZSM5 leads to much higher propane conversion rates than on Zn/H-ZSM5. As the acid site density decreases, propene aromatization rates decrease, which leads to less hydrogen to be disposed by a more efficient hydrogen recombinative desorption species $(ZnOH)^+$.

1. Introduction

The exchange of cations such as Ga,[1–13] Zn,[14–25] or Pt[26–32] into H-ZSM5 increases the rate of non-oxidative propane conversion and the selectivity to unsaturated products. These modifications provide the basis for commercial processes for the conversion of light alkanes to aromatics and hydrogen.[33,34] Several studies have concluded that alkane aromatization on ZSM5 proceeds *via* bifunctional pathways requiring metal cations and Bronsted acid sites, but the catalytic role of the metal cations remains the subject of discussion. Guisnet *et al.*[3,4,8,11] suggested from the higher rate of propene formation on Ga/H-ZSM5 than on H-ZSM5 that Ga cations are involved in initial propane dehydrogenation steps, with the alkenes formed converted to higher hydrocarbons *via* cyclization on Bronsted acid sites in H-ZSM5. They also suggested that these metal cations catalyze the dehydrogenation of naphthene intermediates to aromatics. Mole *et al.*[14] first proposed that metal cations (*e.g.* Zn) in H-ZSM5 were involved in all dehydrogenation steps required for alkane aromatization, but only by catalyzing the recombinative desorption of H-atoms as H_2, while all other steps occurred on acid sites. Ono *et al.*[15] examined the role of metal cations and acid sites in propane reactions on weakly acidic Zn-exchanged borosilicates with pentasil structure. Zn-exchanged borosilicates did not catalyze reactions of propane, but readily converted propene to aromatics. These authors concluded that exchanged Zn species cannot catalyze initial alkane dehydrogenation steps without the concurrent presence of Bronsted acid sites of sufficient strength to activate C–H bonds in propane.

This study addresses the behavior of Zn/Na-ZSM5 catalysts in non-oxidative reactions of propane. The requirement for cations and acid sites in bifunctional reaction pathways suggests that Zn/Na-ZSM5 materials would not convert propane to propene and aromatics because they lack Bronsted acidity. Yet, we report here that propane conversion turnover rates are much higher on Zn/Na-ZSM5 than on Zn/H-ZSM5 or H-ZSM5. Hagen *et al.*[19,21] also measured a higher ethane conversion rate on 0.5% Zn/Na-ZSM5 than on 0.5% Zn/H-ZSM5, without reporting any structural characterization of the materials or an explanation for these effects. Here, we examine mechanistic details and structural requirements for propane reactions on Zn/Na-ZSM5 using kinetic, isotopic tracer and spectroscopic techniques.

2. Experimental methods

2.1 Catalyst synthesis

Zn/Na-ZSM5 catalysts were prepared by aqueous ion-exchange at 343 K for 6 or 24 h using Na-ZSM5 (Zeochem, Si/Al = 14.5) and a solution of $Zn(NO_3)_2$ (0.015 M, Aldrich, >98.0%). Zn/Na-ZSM5 samples were treated in flowing dry air at 383 K for 20 h and then at 773 K for 20 h. NH_4-ZSM5 was prepared by ion-exchange of Na-ZSM5 with a solution of NH_4NO_3 (Fisher, Certified ACS, >98.0%; 0.67 M) at 353 K for 10 h. NH_4^+ exchange was repeated three times using fresh NH_4NO_3 solutions and the samples were then treated in air at 773 K for 24 h in order to form H-ZSM5. Zn/H-ZSM5 was prepared by ion-exchange of H-ZSM5, as reported previously.[25]

2.2 Elemental analysis

Elemental compositions were measured by atomic absorption spectroscopy. The Si/Al atomic ratio was 14.5 ± 0.9 in all

samples. The Zn contents in the two Zn/Na-ZSM5 samples were 1.05 and 2.04 wt.%, corresponding to Zn/Al atomic ratios of 0.18 and 0.36, respectively (Table 1). The Zn content in the ion-exchanged Zn/H-ZSM5 sample was 1.07 wt.% (Zn/Al = 0.17).

2.3 Catalytic reaction studies

Propane reactions were carried out in a gradientless recirculating reactor operated in batch mode.[35] Propane conversion was changed by varying the contact time in the batch reactor. The chemical and isotopic compositions of reactants and products were measured by capillary column gas chromatography using flame ionization and electron-impact mass spectrometric detection (Hewlett Packard 5890/5972, HP-1 methyl-silicone column, 50 m, 0.32 mm diameter, 1.05 μm film thickness). Deuterium contents in reactants and products were determined from mass spectrometric data using matrix techniques that correct for ion fragmentation and isotopic impurities.[36] Isotopic analysis methods have been described in detail elsewhere.[25]

Propane (Matheson, instrument purity, >99.5%) and deuterium (Matheson, chemical purity >99.5%, isotopic purity >99.0%) were used without further purification. Helium (Linde, chemical purity >99.995%) was used as an inert diluent and purified by passage through oxygen removal (Matheson, Oxisorb) and molecular sieve traps (13X and 5A).

Batch reactor data are shown as product site-yields (mole product per g-atom Al) or reactant turnovers (mole C_3H_8 converted per g-atom Al) as a function of contact time. The slope of these plots can be used to calculate product site–time yields or propane conversion turnover rates per Al atom in samples. These values accurately reflect turnover rates only if acid sites are required for rate-determining reaction steps in the bifunctional catalytic sequence and protons are not replaced as Zn or Na cations are exchanged. These values can be converted to turnover rates based on Zn species by dividing them by the (Zn/Al) atomic ratio for each catalyst. Selectivities are reported on a carbon basis, unless noted otherwise.

2.4 Zn-K edge X-ray absorption spectroscopy

The structure and chemical state of Zn species in Zn-containing samples was determined by X-ray absorption measurements at the Zn-K edge using beamline 4-3 at the Stanford Synchrotron Research Laboratory. The beamline details, *in-situ* X-ray absorption cell, and data analysis procedures used have been described in detail elsewhere.[37] Gases were introduced into the X-ray absorption cell using a portable gas handling unit and He, H_2, and C_3H_8 lecture bottles. Helium (Matheson, chemical purity >99.995%) and propane (Matheson, chemical purity >99.5%) were purified using a water trap (Oxyclear, 5A) followed by an oxygen indicating trap (Matheson, Oxisorb). Hydrogen (Matheson, chemical purity >99.99%) was purified by passing through a catalytic purifier (Matheson) and then through a water removal trap (Oxyclear, 5A).

2.5 Isotopic titration of Bronsted acid sites with deuterium

Isotopic exchange between D_2(g) and surface OH species was carried out in a flow apparatus consisting of a metered gas manifold connected to a quartz capillary cell. Samples were heated to 773 K in a flowing H_2–Ar mixture (5.0% H_2, Matheson, certified standard, 100 cm^3 min^{-1}), held isothermal for 2 h, and then cooled to 300 K. The flow was then switched to a D_2–Ar mixture (5.0% D_2, Matheson, certified standard, 100 cm^3 min^{-1}) and the temperature was increased from 300 K to 1073 K at 10 K min^{-1}. The H_2, HD, and D_2 concentrations in the effluent were measured by on-line mass spectrometry (Leybold-Inficon, Model THP TS200).

2.6 Temperature programmed reduction

Temperature programmed reduction (TPR) experiments were carried out using a Quantasorb apparatus (Quantachrome, Inc.) modified with a programmable furnace. Samples were held within a quartz cell and flushed with N_2 (Matheson, chemical purity >99.998%, 50 cm^3 min^{-1}) at room temperature for 0.5 h before reduction. TPR was carried out using a H_2–Ar mixture (21.0% H_2, Matheson, certified standard, 80 cm^3 min^{-1}) and a temperature ramp of 10 K min^{-1} from room temperature to 1073 K. The effluent stream was passed through a 13X molecular sieve trap in order to remove the water formed during reduction. The H_2 concentration in the effluent was measured using a thermal conductivity detector. The detector output was calibrated using the reduction of bulk WO_3 powder (Aldrich, 99.99%, treated in O_2 for 3 h at 973 K).

3. Results and discussion

3.1 The effect of Zn on propane conversion rates (H-ZSM5 and Na-ZSM5)

Propane conversion turnovers on Na-ZSM5 and H-ZSM5 catalysts are significantly lower than on Zn/H-ZSM5 (Fig. 1). When Zn is exchanged into H-ZSM5, dehydrogenated products form with higher selectivity and the C_1–C_2 yields decrease (Table 2). This beneficial effect of Zn was first reported by Mole *et al.*[14] and later confirmed by many other researchers.[15-25]

Zn exchange also leads to an increase in the rate of H_2 formation (Fig. 2). On H-ZSM5, the H_2 selectivity is low (4.6%), but the addition of Zn (1.07 wt.%) increases H_2 selec-

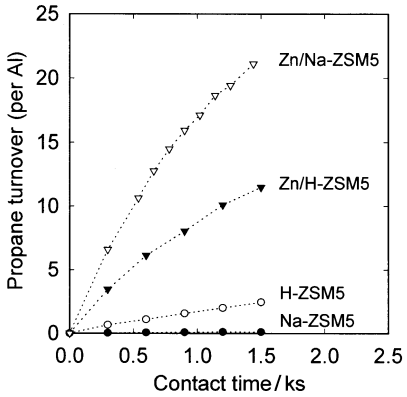

Fig. 1 Propane turnover *vs.* contact time during propane conversion on Na-ZSM5, H-ZSM5, 1.07 wt.% Zn/H-ZSM5, and 1.05 wt.% Zn/Na-ZSM5 (773 K, 26.6 kPa C_3H_8, 74.7 kPa He).

Table 1 Elemental analysis results of Zn/H-ZSM5 and Zn/Na-ZSM5

Sample	Zn (wt.%)	Amount/mmol g^{-1} Zn	Al	Na	Zn/Al
Zn/Na-ZSM5	1.05	0.16	0.87	0.58	0.18
Zn/Na-ZSM5	2.04	0.31	0.86	0.23	0.36
Zn/H-ZSM5	1.07	0.16	0.89	0.01	0.17

Table 2 Propane turnover rates and product distribution on H-ZSM5, Zn/H-ZSM5 and Zn/Na-ZSM5 (773 K, 26.6 kPa C_3H_8, 74.7 kPa He)

Zn (wt.%)	H-ZSM5 (0.00)	Zn/H-ZSM5 (1.07)	Zn/Na-ZSM5 (1.05)	Zn/Na-ZSM5 (2.04)
Zn/Al	0.00	0.17	0.18	0.36
Propane conversion (%)	7.6	7.6	7.7	7.5
Propane turnover rate (per Al)/10^{-3} s^{-1}	1.7	4.7	19.3	27.9
Propene formation rate (per Al)/10^{-3} s^{-1}	0.4	1.6	13.7	13.3
Aromatization site–time yield (per Al)/10^{-3} s^{-1}	0.1	1.6	2.7	7.5
Carbon selectivity (%)				
Methane	23.2	7.0	1.5	3.8
Ethene	33.2	14.9	3.9	7.0
Ethane	7.3	6.2	3.7	8.4
Propene	22.4	33.7	71.1	47.5
C_{6+} aromatics	2.4	33.5	13.9	26.8
Benzene	0.8	15.2	6.7	12.3
Toluene	1.5	13.0	4.7	9.9
C_{8+}	0.1	5.3	2.5	4.6
Hydrogen selectivity (%)				
Hydrogen (H_2)	4.6	29.0	32.4	28.2

tivity (29.0%) (Table 2). These Zn cations provide an alternate hydrogen removal path by catalyzing the recombinative desorption of hydrogen as H_2.[22,25] As a result, Zn increases the rate of propane conversion to unsaturated products.

Previous reports have concluded that weakly acidic Zn-exchanged borosilicates (Zn/H-[B]-ZSM5) are not active in propane conversion reactions,[15] suggesting that Zn species, by themselves, cannot catalyze the required initial dehydrogenation of propane in the absence of strong Bronsted acid sites. In view of this, Zn/Na-ZSM5, which nominally lacks Bronsted acid sites, should be inactive for propane reactions. Propane conversion turnover rates and propene formation rates, however, are much higher on Zn/Na-ZSM5 (1.05 wt.%) than on Zn/H-ZSM5 (1.07 wt.%) or H-ZSM5 (Table 2, Fig. 1).

Selectivities during propane conversion are markedly different on Zn/H-ZSM5 (1.07 wt.%) and Zn/Na-ZSM5 (1.05 wt.%) catalysts. At the same conversion level, the predominant products on Zn/H-ZSM5 are C_{6+} aromatics (33.5%) and propene (33.7%) (Table 2; 7.5–7.7% conversion), but propene is the main product on Zn/Na-ZSM5 (71.1%). The aromatic selectivity is lower on Zn/Na-ZSM5 than on Zn/H-ZSM5, because chain growth and cyclization pathways require Bronsted acid sites. The formation of C_{3+} products on Zn/Na-ZSM5 suggests, however, that some Bronsted acid sites are present in these samples, although at much lower concentrations than in Zn/H-ZSM5. Increasing the Zn loading in Zn/Na-ZSM5 from 1.05 to 2.04 wt.% increases propane conversion rates (from 19.3×10^{-3} to 27.9×10^{-3} s^{-1}) and aromatics selectivity

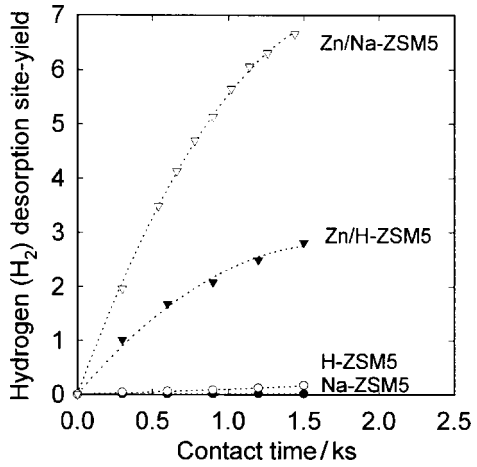

Fig. 2 Hydrogen (H_2) desorption site-yield *vs.* contact time during propane conversion of Na-ZSM5, H-ZSM5, 1.07 wt.% Zn/H-ZSM5 and 1.05 wt.% Zn/Na-ZSM5 (773 K, 26.6 kPa C_3H_8, 74.7 kPa He).

(from 13.9 to 26.8%) at similar propane conversions (7.5–7.7%) (Table 2). This increase in aromatic yield with increasing Zn content suggests that residual protons may be formed during Zn exchange into Na-ZSM5; as a result, increasing the Zn content increases the concentration of protons in Zn/Na-ZSM5.

Propene formation rates are significantly higher on Zn/Na-ZSM5 (1.05 wt.%; 13.7×10^{-3} s^{-1}) than on Zn/H-ZSM5 (1.07 wt.%; 1.6×10^{-3} s^{-1}) (Table 2). In contrast with our previous results on Zn/H-ZSM5,[25] an increase in Zn loading on Zn/Na-ZSM5 did not increase propene formation rates ($\sim 13.5 \times 10^{-3}$ s^{-1}) (Table 2). The extent to which propane dehydrogenation approaches equilibrium may be estimated by calculating the value of η, defined as

$$\eta = (C_3H_6)(H_2)/(C_3H_8)K,$$

in which the concentrations are those at a given conversion in the gas phase contacting the catalyst and K is the equilibrium constant for propane dehydrogenation at 773 K. The value of η would approach unity at thermodynamic equilibrium; it is much lower than one, however, at all reaction conditions of this study ($\eta = 0.16$ on 1.05 wt.% Zn/Na-ZSM5 at 7.5% propane conversion), indicating that the propane dehydrogenation step is far from equilibrium on Zn/Na-ZSM5 catalysts.

Increasing the Zn content in Zn/Na-ZSM5 did not increase propene formation rates because as the Zn loading is increased, the rate of conversion of propene to aromatics also increases, suggesting that more protons are generated during synthesis at higher Zn loadings. This higher proton concentration in 2.04 wt.% Zn/Na-ZSM5 leads to higher propene consumption rates and to a propane product distribution similar to that in Zn/H-ZSM5 (Table 2). Higher Zn loadings in Zn/Na-ZSM5 increase the total propane conversion rate, but the increase is not proportional to the amount of Zn.

3.2 Characterization of Zn/Na-ZSM5 using X-ray absorption spectroscopy

Near-edge and fine structure analyses of X-ray absorption spectra at the Zn-K edge were used to determine the oxidation state and the local structure of exchanged Zn cations in Zn/Na-ZSM5. X-ray absorption spectroscopy is an element-specific technique that can probe the local structure around absorber atoms at typical conditions of catalyst pretreatment and catalytic reactions. Spectral features near the absorption edge can be used to determine the symmetry and oxidation

state of the absorber by comparing them with those in the spectra of compounds with known structure.[38,39] The absorption edge energy depends on the oxidation state of Zn species; Zn-K edges shift to higher energy during oxidation of Zn^0 to Zn^{2+}.[40] On Zn/Na-ZSM5 samples (1.05 and 2.04 wt.% Zn), absorption edge energies were not influenced by H_2 or He treatments at 773 K or by C_3H_8 reactions at 773 K. These absorption edge energies are very similar to those in ZnO (7884.4 eV on ZnO *vs.* 7884.4 eV on Zn/Na-ZSM5) suggesting that Zn/Na-ZSM5 contains predominantly Zn^{2+} cations. These cations do not reduce to Zn^0 during reactions of alkanes at 773 K. Similar conclusions were reached previously for Zn cations in Zn/H-ZSM5.[37]

Radial distribution functions obtained from extended X-ray absorption fine structure (EXAFS) measurements at the Zn-K edge for Zn/NaZSM5, Zn/H-ZSM5, Zn foil, and ZnO powders were used to determine the position and number of Zn and O neighbors around Zn^{2+} cations (Fig. 3). The peak at 1.5 Å in ZnO powders arises from scattering by the electron cloud of oxygen atoms directly bonded to Zn. This peak is also present in the radial distribution functions of both Zn/Na-ZSM5 samples, confirming the presence of oxidized Zn. Zn/Na-ZSM5 radial distribution functions do not contain a peak at 2.3 Å, corresponding to Zn–Zn nearest neighbors in Zn foil, or a peak at 3.0 Å, characteristic of Zn–Zn next nearest neighbors in ZnO (Fig. 3). Therefore, Zn^{2+} centers are not present as ZnO crystallites in Zn/Na-ZSM5 samples. Zn^{2+} species are isolated and contain few next nearest neighbors, as expected if they were present at cation exchange sites. Similar results were reported previously for Zn/H-ZSM5 (Fig. 3).[37] The Al or Si next nearest neighbors expected for Zn cations at exchange sites (Zn–O–Al or Zn–O–Si) are not seen in the radial distribution function of Zn/Na-ZSM5 or Zn/H-ZSM5 because of unconstrained vibrations and a range of Zn local geometries at cation exchange sites. These neighbors do not appear to be well-ordered with respect to the absorbing Zn atom.

3.3 Temperature programmed reduction of Zn/Na-ZSM5

Previous TPR studies showed that exchanged Zn^{2+} species in Zn/H-ZSM5 do not reduce below 1173 K,[37] apparently because framework oxygens in ZSM5 stabilize Zn^{2+} cations. Also, stable metal nuclei cannot form from isolated cations without significant migration of Zn species, thus weakening the thermodynamic incentive for reduction to Zn metal. Although X-ray diffraction data suggest that the ZSM5 zeolite structure starts to collapse at temperatures above 973 K, it appears that these Zn cations remain anchored at exchange sites during this process. TPR studies showed that Zn^{2+} species in Zn/Na-ZSM5 reduce more easily than in Zn/H-ZSM5 (Fig. 4). This reduction of Zn in Zn/Na-ZSM5 (1.05 and 2.04 wt.%) starts at about 800 K (Fig. 4) and it suggests that Zn^{2+} species in Zn/Na-ZSM5 catalyze H_2 dissociation and undergo reduction more efficiently than the corresponding Zn^{2+} cations in Zn/H-ZSM5.[37] H_2 uptakes (mole H_2 consumed per g-atom Zn) during reduction are 0.99 for Zn/Na-ZSM5 (1.05 wt.%) and 0.77 for Zn/Na-ZSM5 (2.04 wt.%). The H_2/Zn ratio on 2.04 wt.% Zn/Na-ZSM5 is smaller than the value of unity expected for full reduction to Zn^0, suggesting that, unlike 1.05 wt.% Zn/Na-ZSM5, this sample contains both reducible and unreducible Zn species.

Previous studies of the density and the local structure of exchanged Zn cations in Zn/H-ZSM5 showed that $(ZnOH)^+$ species initially form at exchange sites during ion-exchange from aqueous nitrate solutions.[24,37,41] In Zn/H-ZSM5, these $(ZnOH)^+$ species interact initially with one Al site and replace one proton during exchange. $(ZnOH)^+$ is also expected to form during exchange of Na-ZSM5 by replacement of one Na^+ cation. The presence of H^+ ions in aqueous nitrate solutions (pH 6.2–6.8), however, can lead to the concurrent replacement of some Na^+ with H^+ during Zn exchange.

At higher temperatures, $(ZnOH)^+$ species in Zn/H-ZSM5 with low Zn content (Zn/Al <0.2 at.) react predominantly with neighboring OH groups to form water and Zn^{2+} cations bridging two exchange sites (O^-–Zn^{2+}–O^-). This stoichiometry has been confirmed using NH_3 titration,[37] isotopic titration of surface OH groups with D_2,[37] and by the reduction of Zn^{2+} with CO[24] for Zn/H-ZSM5. Both analytical[42] and computational[43] studies of Al statistics in ZSM5 (Si/Al = 14.5) indicate a large fraction of Al T sites (0.546,[42] 0.568[43]) have Al next-nearest neighbors (NNN). On Zn/Na-ZSM5 (1.05 wt.%), this dehydration will occur rarely, if at all, because Na^+ occupies most of the neighboring Al sites (Na/Al = 0.58). Consequently, Zn species in Zn/Na-ZSM5 (1.05 wt.%) appear to remain as $(ZnOH)^+$ during propane conversion. These Na cations can prevent the conversion of $(ZnOH)^+$ into (O^-–Zn^{2+}–O^-). It is possible that at higher Zn loadings, $(ZnOH)^+$ species combine with nearby $(ZnOH)^+$ to form water and another Zn^{2+} species, a process by which two Zn cations form a (O^-–Zn^{2+}–O–Zn^{2+}–O^-) dimer interacting

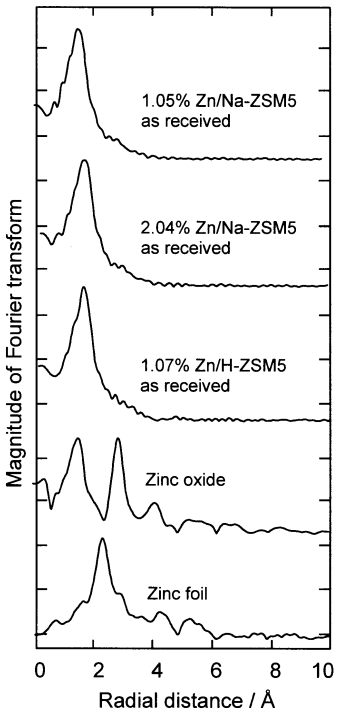

Fig. 3 EXAFS Zn-K edge radial distribution functions for fresh Zn/Na-ZSM5, Zn/H-ZSM5, ZnO and Zn foil.

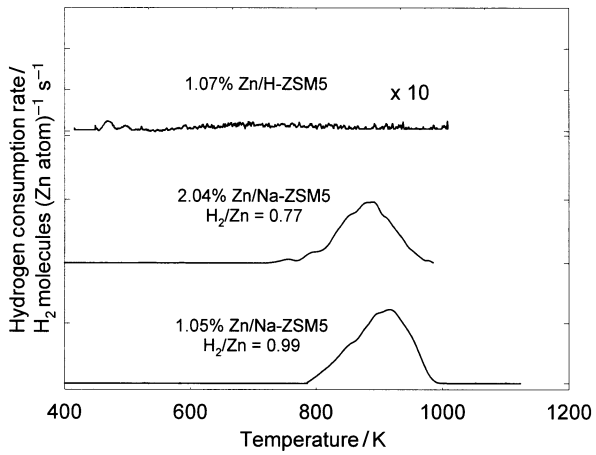

Fig. 4 Temperature programmed reduction of 1.07 wt.%. Zn/H-ZSM5, 1.05 wt.% Zn/Na-ZSM5 and 2.04 wt.% Zn/Na-ZSM5 (80 cm^3 min^{-1}, 21% H_2–Ar, 10 K min^{-1}).

with two Al exchange sites. These dimer species may be less active for propane conversion than $(ZnOH)^+$ species and explain why higher Zn loading Zn/Na-ZSM5 (2.04 wt.%) catalysts are not proportionally more active for propane conversion and propene formation than in the Zn/Na-ZSM5 with the lower Zn content (1.05 wt.%) (Table 2). These (O^-–Zn^{2+}–O–Zn^{2+}–O^-) dimer species, however, should show evidence of Zn next nearest neighbors in the XAS radial structure function, but experimental spectra fail to show Zn next nearest neighbors (Fig. 3) on Zn/Na-ZSM5. This suggests that the concentration of these dimer species is small or that features corresponding to these Zn dimers are not seen in the radial distribution function.

The amount of H_2 consumed per Zn atom during temperature programmed reduction suggests that $(ZnOH)^+$ species (reducible at about 800 K) and unreducible (O^-–Zn^{2+}–O^-) or (O^-–Zn^{2+}–O–Zn^{2+}–O^-) species co-exist in Zn/Na-ZSM5. Stabilized (O^-–Zn^{2+}–O^-) species do not reduce even at 1100 K, but $(ZnOH)^+$ species in Zn/Na-ZSM5 start to reduce at 800 K. The H_2/Zn ratio for 1.05 wt.% Zn/Na-ZSM5 (0.99) shows that most of the Zn atoms are present as reducible $(ZnOH)^+$ species. On the 2.04 wt.% Zn/Na-ZSM5 sample, only 77% of the Zn cations are present as reducible $(ZnOH)^+$ species and the rest as unreducible (O^-–Zn^{2+}–O^-) or (O^-–Zn^{2+}–O–Zn^{2+}–O^-).

3.4 Isotopic titration of Bronsted acid sites with deuterium

The formation of aromatics during propane conversion requires the presence of Bronsted acid sites, which catalyze chain growth and cyclization of intermediate alkenes. The observed presence of aromatics among the products of propane reactions on Zn/Na-ZSM5 shows that Bronsted acid sites must form during exchange of Na-ZSM5 with Zn^{2+} ions in solution. D_2 exchange with zeolite OH groups was used to measure the number of residual hydroxyl groups in Zn/Na-ZSM5 samples. This method counts the number of exchangeable H-atoms irrespective of their location (as Zn-OH, silanol or acidic hydroxyl groups). Our previous measurements on H-ZSM5 showed that D_2 dissociates and exchanges with surface H-atoms at 600–1000 K to give 1.04 H atoms per Al site.[37] Novakova *et al.* used infrared spectroscopy to show that during isotopic exchange with D_2, deuterium replaces both protons and silanol groups in Y zeolite.[44] Thus the number of surface H-atoms equals the number of Bronsted acid sites, as long as silanol groups are minority species.

The temperature required for D_2–OH exchange decreases as Zn cations introduce D_2 dissociative chemisorption sites. On Zn/H-ZSM5 (1.07 wt.%), D_2 dissociates and exchanges with surface OH groups at lower temperatures (475–550 K) than on H-ZSM5 (600–1000 K) (Fig. 5). D_2 exchange gives 0.74 H atoms per Al site on this Zn/H-ZSM5 (Zn/Al = 0.17),

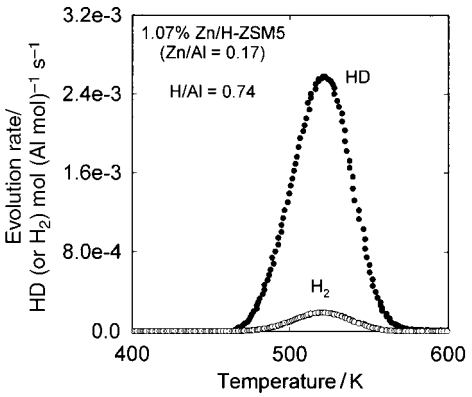

Fig. 5 HD and H_2 evolution rate as a function of temperature during isotopic exchange with D_2 on 1.07 wt.% Zn/H-ZSM5 (Zn/Al = 0.17) (5% D–Ar, 80 cm^3 min^{-1}, 10 K min^{-1}).

as expected from the occupation of all A1 sites by either (O^-–Zn^{2+}–O^-) or H^+.

Isotopic exchange measurments were also carried out on Zn/Na (1.05 wt.%, Zn/Al = 0.18 and 2.04 wt.%, Zn/Al = 0.36) in order to determine the density of remaining OH groups. If OH groups associated with Al sites in the zeolite were not present, D_2 would exchange only with H-atoms in $(ZnOH)^+$ species and the resulting exchange would correspond to the density of reducible Zn species in the sample (*e.g.* 0.18 H/Al for 1.05 wt.% Zn/Na-ZSM5). Isotopic measurements on Na-ZSM5 showed no D_2–OH exchange, suggesting that the initial zeolite does not contain protons. On the 1.05 wt.% Zn/Na-ZSM5 sample, the number of hydrogen atoms exchanged (measured from the area under the HD and H_2 peaks) corresponds to 0.45 H atoms per Al site (Table 3). This value is significantly higher than expected from the number of reducible $(ZnOH)^+$ moieties in Zn/Na-ZSM5 (1.05 wt.%, Zn/Al = 0.18). Similar isotopic measurements on Zn/Na-ZSM5 samples with higher Zn content (2.04 wt.%, Zn/Al = 0.36) led to even higher OH densities (0.71 H/Al, Table 3). These exchange data suggest that protons are formed in Zn/Na-ZSM5 during Zn exchange or catalyst pre-treatment, a conclusion consistent with the formation of aromatics *via* acid-catalyzed chain growth and cyclization during propane conversion (Table 2). Ammonia desorption experiments suggest that these minority protons in Zn/Na-ZSM5 have similar acid strength to those protons found in Zn/H-ZSM5 and H-ZSM5. The higher proton density in 2.04 wt.%, Zn/Na-ZSM5 leads to higher aromatic selectivities during propane conversion than on 1.05 wt.% Zn/Na-ZSM5 (Table 2).

Thus, Zn/Na-ZSM5 (1.05% wt., Zn/Al = 0.18) contains approximately 0.18 $(ZnOH)^+$ (from elemental analysis) and 0.27 H^+ (from D_2–OH exchange data; 0.45 total H/Al − 0.18 $ZnOH^+$/Al) (Table 4). The remaining sites must be occupied by Na cations, leading to a balance of 0.55 Na per Al. This value is similar to the Na content measured by atomic absorption (Na/Al = 0.58) (Table 1).

TPR data on Zn/Na-ZSM5 (2.04 wt.%, Zn/Al = 0.36) suggest that unlike 1.05 wt.%, Zn/Na-ZSM5, the sample with the higher Zn content contains several different types of Zn species (reducible $(ZnOH)^+$; unreducible (O^-–Zn^{2+}–O^-) or (O^-–Zn^{2+}–O–Zn^{2+}–O^-) species). Unreducible (O^-–Zn^{2+}–O^-) species can form *via* condensation of $(ZnOH)^+$ and H^+, while (O^-–Zn^{2+}–O–Zn^{2+}–O^-) can form *via* similar reactions

Table 3 Isotopic exchange results of OH groups with deuterium on Zn/H-ZSM5 and Zn/Na-ZSM5 (5% D_2–Ar, 80 cm^3 min^{-1}, 10 K min^{-1})

Sample	Zn (wt.%)	H atoms/Al site
H-ZSM5	0	1.04
Zn/H-ZSM5	1.07	0.74
Zn/Na-ZSM5	1.05	0.45
Zn/Na-ZSM5	2.04	0.71

Table 4 Concentration of different species present in Zn/Na-ZSM5 (1.05 wt.%)

	Number of cations/Al site
$ZnOH^+$	0.18[a]
H^+	0.27[b]
Na^+	0.55[c]

[a] From elemental analysis. [b] 0.45 H (from D_2–OH) − 0.18 H (from $ZnOH^+$). [c] 1.0 − H^+ − $ZnOH^+$.

between two nearby $(ZnOH)^+$ species, which increase in surface density with increasing Zn content.

Similar calculations on Zn/Na-ZSM5 (2.04 wt.%, Zn/Al = 0.36) are more difficult to interpret because of the many possible species that can co-exist at higher Zn loadings. If the concentration of $(O^-–Zn^{2+}–O^-)$ is negligible, the sample contains approximately 0.27 $(ZnOH)^+$, 0.44 H^+, and 0.09 $(O^-–Zn^{2+}–O^-–Zn^{2+}–O^-)$ cations per Al site (the Zn speciation was calculated from the amount of Zn (77%) that reduces below 1100 K during TPR). The remaining sites must be occupied by Na^+ cations, leading to a balance of 0.11 Na per Al. This value differs, however, from that measured by elemental analysis (Na/Al = 0.23) suggesting that some $(O^-–Zn^{2+}–O^-)$ species must also be present in Zn/Na-ZSM5 (2.04 wt.%) along with $(O^-Zn^{2+}–O^-Zn^{2+}–O^-)$ groups.

Higher Zn contents appear to lead to higher Bronsted acid site densities and thus, explain the higher aromatics formation rate and aromatic selectivities on 2.04 wt.% Zn/Na-ZSM5 than on 1.05 wt.% Zn/Na-ZSM5 (Table 2). These Bronsted acid sites arise from protons present in the acidic Zn nitrate solution or from NH_4NO_3 impurities in $Zn(NO_3)_2$. For higher Zn loadings, a longer solution time was used, therefore increasing the probability of proton formation in Zn/Na-ZSM5.

Characterization studies of Zn/H-ZSM5 and Zn/Na-ZSM5 suggest that different Zn species are present during high temperature treatments. $(ZnOH)^+$ species at cation exchange positions are the initial species formed during Zn ion exchange with Na-ZSM5 and H-ZSM5. At low Si/Al ratios, these $(ZnOH)^+$ species can undergo condensation reactions with neighboring H^+ or $(ZnOH)^+$ to form more stable $(O^-–Zn^{2+}–O^-)$ or $(O^-–Zn^{2+}–O^-–Zn^{2+}–O^-)$ species respectively. These more stable Zn species are less active during propane reactions than $(ZnOH)^+$.

3.5 Hydrogen removal pathways on Zn/Na-ZSM5

The temperature required to form HD during D_2–OH exchange is slightly lower on Zn/Na-ZSM5 (1.05 wt.% Zn) than on Zn/H-ZSM5 (1.07 wt.% Zn) (Fig. 6), because $(ZnOH)^+$ species appear to dissociate D_2 more effectively than $(O^-–Zn^{2+}–O^-)$ species present in Zn/H-ZSM5. These data do not provide, however, a direct measure of hydrogen dissociation–recombination during propane conversion reactions. Thus, the reversibility of hydrogen adsorption–desorption steps during propane conversion was determined from the deuterium content in the products formed from C_3H_8–D_2 reaction mixtures. Hydrogen removal as H_2 after C–H bond activation is a kinetically relevant and nearly irreversible step in propane aromatization reactions on H-ZSM5 and Zn/H-ZSM5.[7,9,22,25] In the absence of recombinative desorption sites, H-atoms are removed more slowly by alternate pathways, such as hydrogenation of alkenes and other unsaturated surface species to form methane and ethane as preferred products.

On H-ZSM5, the deuterium fraction within all reaction products of C_3H_8–D_2 mixtures is very low (0.03) and it is independent of contact time or conversion (Fig. 7).[7,9,22,25] The deuterium distribution in each product obeys the binomial equation. Therefore, the surface hydrogen pool is sampled statistically by all products formed and it contains approximately 3% deuterium and 97% protium, instead of only D-atoms, the result expected from quasi-equilibrated hydrogen adsorption–desorption steps. The removal of protium atoms formed during C–H activation is irreversible and limits the rate of the initial dehydrogenation steps required for propane conversion reactions on H-ZSM5.

On Zn/H-ZSM5 (1.07 wt.% Zn), the deuterium atoms are also statistically distributed and the deuterium content similar in all products of C_3H_8–D_2 reactions. The deuterium fraction in all products (extrapolated to zero conversion to account for the increasing concentration of HD and H_2 in the initially pure D_2 gas phase) is much higher (0.22) than on H-ZSM5 (0.03) (*e.g.* toluene, Fig. 7). Active Zn species in Zn/H-ZSM5 provide H-atom recombination sites and, as a result, increase the reversibility of H-atom adsorption–desorption steps and the rates of both propane conversion to aromatics and of hydrogen desorption steps.[7,9,22,25]

The deuterium content within products of C_3H_8–D_2 mixtures on Zn/Na-ZSM5 (1.05 wt.% Zn) is even higher (0.26) than on Zn/H-ZSM5 (0.22) (*e.g.* toluene, Fig. 7). This higher deuterium content suggests that Zn species in Zn/Na-ZSM5 catalyze D_2 dissociative adsorption more efficiently than Zn species in Zn/H-ZSM5. Higher recombinative desorption rates lead to higher deuterium (and hydrogen) removal rates during propane conversion (Fig. 2) and faster propane dehydrogenation and aromatization reactions. This increase in deuterium concentration is unlikely to account by itself for the four-fold increase in propane conversion.

The unexpected increase in propane conversion turnover rates when Zn/Na-ZSM5 is prepared by Zn exchange into Na-ZSM5 instead of H-ZSM5 appears to be a combination of two factors, the higher hydrogen recombination efficiency on the Zn species in Zn/Na-ZSM5 and the lower number of acid sites in Zn/Na-ZSM5. The deuterium content in the products of C_3H_8–D_2 mixtures showed that Zn species found in Zn/Na-ZSM5 are more efficient in the recombinative desorption of H-atoms than $(O^-–Zn^{2+}–O^-)$ species in Zn/H-ZSM5. Hydrogen recombination has been shown to be the rate-determining step during propane conversion.[7,9,22,25] When

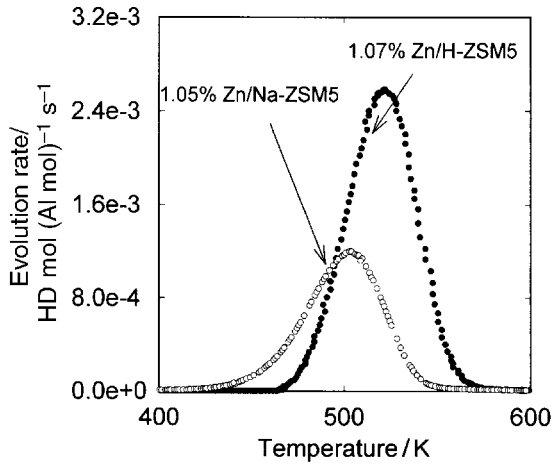

Fig. 6 Comparison of HD evolution rate during isotopic exchange with D_2 on 1.05 wt.% Zn/Na-ZSM5 and 1.07 wt.% Zn/H-ZSM5 (5% D_2–Ar, 80 cm^3 min^{-1}, 10 K min^{-1}).

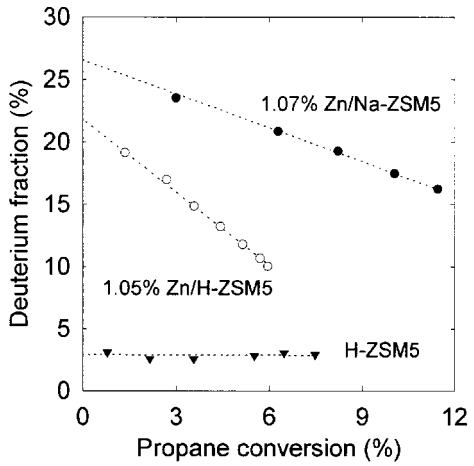

Fig. 7 Deuterium fraction in toluene products of propane–deuterium mixtures on H-ZSM5, Zn/H-ZSM5 and Zn/Na-ZSM5 (773 K, 26.6 kPa C_3H_8, 6.7 kPa D_2, 68.0 kPa He).

Na cations are present, the total number of protons and the rate of chain growth decreases, which shifts the propane product distribution from aromatics to propene. Thus, the total amount of hydrogen that must be removed from the surface is much less to form propene than to form a more unsaturated benzene molecule. Hydrogen selectivities are similar in all Zn catalysts, but the excess hydrogen that must be disposed as aromatics are produced in Zn/H-ZSM5 and Zn/Na-ZSM5 (2.04 wt.%) leads to the unselective removal of hydrogen, as methane and ethane (Table 2). The propane rate does not increase linearly with Zn loading in Zn/Na-ZSM5 because less active Zn species are formed and because the sample contains a higher proton concentration. The higher proton site density leads to higher propene aromatization rates, which leads to more H-atoms to be disposed, causing Zn/Na-ZSM5 to resemble Zn/H-ZSM5.

4. Conclusions

Propane reactions on Zn/Na-ZSM5 lead to higher propane turnover rates and propene selectivities than on Zn/H-ZSM5 or H-ZSM5. The increase in propane conversion turnover rates on Zn/Na-ZSM5 appears to be attributed to the increase of the rate of hydrogen desorption and a lower acid site density. Isotopic exchange of surface OH groups with D_2 suggests that protons form during Zn exchange onto Na/ZSM5. These Bronsted acid sites are responsible for acid-catalyzed chain growth and cyclization reactions. Zn/Na-ZSM5 (1.05 wt.%) has a lower Bronsted acid concentration than H-ZSM5 and 1.07 wt.% Zn/H-ZSM5; this residual proton concentration results in lower aromatic selectivities on Zn/Na-ZSM5.

In-situ Zn-K edge X-ray absorption studies show that aqueous ion exchange with Na-ZSM5 leads to isolated Zn^{2+} species residing at cation exchange sites. Similar to exchange with H-ZSM5, direct ion exchange of Na-ZSM5 with Zn nitrate solutions leads to the presence of $(ZnOH)^+$ species. However, Na cations prevent Zn from dehydrating with nearby OH groups as found previously in Zn/H-ZSM5, and instead remain as Na^+ and $(ZnOH)^+$.

The deuterium content in reaction products of C_3H_8–D_2 mixtures is higher on 1.05 wt.% Zn/Na-ZSM5 than on 1.07 wt.% Zn/H-ZSM5 and H-ZSM5 suggesting that $(ZnOH)^+$ species are more effective than (O^-–Zn^{2+}–O^-) sites in catalyzing H-atom recombinative desorption. TPR studies indicate that $(ZnOH)^+$ species reduce more easily than (O^-–Zn^{2+}–O^-) species. This ease of reduction and the lower temperatures required for D_2–OH exchange suggest that Zn species in Zn/Na-ZSM5 provide evidence for a more effective hydrogen adsorption–desorption function during propane conversion on these materials.

5. Acknowledgements

This work was supported by the National Science Foundation (CTS-96-13632) and by start-up funds provided by the University of California. X-ray absorption data were collected at Stanford Synchrotron Radiation Laboratory (SSRL), which is operated by the Department of Energy (DOE), Office of Basic Energy Sciences, under contract DE-ACO3-76SF00515. The authors acknowledge Dr George D. Meitzner (Edge Analytical, Inc.) for helpful discussions and expert technical assistance in the analysis of X-ray absorption data.

References

1 H. Kitagawa, Y. Sendoda and Y. Ono, *J. Catal.*, 1986, **101**, 12.
2 T. Yashima, T. Sasaki, K. Takahashi, S. Watanabe and S. Namba, *Sekiyu Gakkaishi*, 1988, **31**, 154.
3 N. S. Gnep, J. Y. Doyemet and M. Guisnet, *J. Mol. Catal.*, 1988, **45**, 281.
4 N. S. Gnep, J. Y. Doyemet, A. M. Seco, F. Ramoa and M. Guisnet, *Appl. Catal.*, 1988, **43**, 155.
5 J. Yao, R. le van Mao and L. Dufresne, *Appl. Catal.*, 1990, **65**, 175.
6 G. L. Price and V. Kanazirev, *J. Catal.*, 1990, **120**, 267.
7 E. Iglesia, J. E. Baumgartner and G. L. Price, *J. Catal.*, 1992, **134**, 549.
8 M. Guisnet, N. S. Gnep and F. Alario, *Appl. Catal.*, 1992, **89**, 1.
9 G. D. Meitzner, E. Iglesia, J. E. Baumgartner and E. S. Huang, *J. Catal.*, 1993, **140**, 209.
10 P. Meriaudeau and C. Naccache, *Catal. Today*, 1996, **31**, 265.
11 M. Guisnet and N. S. Gnep, *Catal. Today*, 1996, **31**, 275.
12 K. M. Dooley, G. L. Price, V. I. Kanazirev and V. I. Hart, *Catal. Today*, 1996, **31**, 305.
13 I. Nakamura and K. Fujimoto, *Catal. Today*, 1996, **31**, 335.
14 T. Mole, J. R. Anderson and G. Creer, *Appl. Catal.*, 1985, **17**, 141.
15 M. Shibata, H. Kitagawa, Y. Sendoda and Y. Ono, in *Proceedings of the 7th International Zeolite Conference*, Elsevier, Tokyo, 1986, p. 717.
16 Y. Ono and K. Kanae, *J. Chem. Soc., Faraday Trans.*, 1991, **87**, 669.
17 F. Roessner, A. Hagen, U. Mroczek, H. G. Karge and K. H. Steinberg, in *Proceedings of the 10th International Congress on Catalysis*, ed. L. Guczi, F. Solymosi and P. Tetenyi, Elsevier, Budapest, 1992, p. 1707.
18 Y. Ono, *Catal. Rev.-Sci. Eng.*, 1992, **34**, 179.
19 A. K. Hagen and F. Roessner, *Stud. Surf. Sci. Catal.*, 1994, **83**, 313.
20 A. Hagen, F. Roessner and W. Reschetilowski, *Chem. Eng. Technol.*, 1995, **18**, 414.
21 A. K. Hagen, O. P. Keipert and F. Roessner, *Stud. Surf. Sci. Catal.*, 1996, **101**, 781.
22 J. A. Biscardi and E. Iglesia, *Catal Today*, 1996, **31**, 207.
23 H. Berndt, G. Lietz, B. Lucke and J. Volter, *Appl. Catal.*, 1996, **146**, 351.
24 H. Berndt, G. Lietz and J. Volter, *Appl. Catal.*, 1996, **146**, 365.
25 J. A. Biscardi and E. Iglesia, *J. Catal.*, 1999, **182**, 117.
26 T. Inui and F. Okazumi, *J. Catal.*, 1984, **90**, 366.
27 C. W. R. Engelen, J. P. Wolthuizen and J. H. C. van Hooff, *Appl Catal.*, 1985, **19**, 153.
28 C. W. R. Engelen, J. P. Wolthuizen, J. H. C. van Hooff and H. W. Zandbergen, *Stud. Surf. Sci. Catal.*, 1986, **28**, 709.
29 N. S. Gnep, J. Y. Doyemet, A. M. Seco, F. R. Ribeiro and M. Guisnet, *Appl. Catal.*, 1987, **35**, 93.
30 K. H. Steinberg, U. Mroczek and F. Roessner, *Appl. Catal.*, 1990, **66**, 37.
31 U. Mroczek, K. H. Steinberg and F. Roessner, *React. Kinet. Catal. Lett.*, 1991, **44**, 201.
32 B. S. Kwak, W. M. H. Sachtler and W. O. Hagg, *J. Catal.*, 1994, **149**, 465.
33 J. A. Johnson and G. K. Hilder, *Proceedings of the NPRA Annual Meeting*, Dallas, TX, AM-84-45, 1984.
34 J. R. Mowry, R. F. Anderson and J. A. Johnson, *Oil Gas J.*, 1985, **83**, 128.
35 J. A. Biscardi and E. Iglesia, *J. Phys. Chem.*, 1998, **102**, 9284.
36 G. L. Price and E. Iglesia, *Ind. Eng. Chem. Res.*, 1989, **28**, 839.
37 J. A. Biscardi, G. D. Meitzner and E. Iglesia, *J. Catal.*, 1998, **179**, 192.
38 F. W. Lytle, G. H. Via and J. H. Sinfelt, *Synchrotron Radiation Research*, Plenum Publications, New York, 1980, 401.
39 F. W. Lytle, in *Applications of Synchrotron Radiation.* Gordon and Breach, Beijing, 1988.
40 V. Kunzl, *Collect. Czech. Chem. Commun.*, 1932, **4**, 213.
41 V. B. Kazansky, L. M. Kustov and A. Y. Khodakov, *Stud. Surf. Sci. Catal.*, 1989, **28**, 1173.
42 M. H. W. Sonnemans, C. den Heijer and M. Crocker, *J. Phys. Chem.*, 1993, **97**, 440.
43 M. J. Rice, A. K. Chakraborty and A. T. Bell, *J. Catal.*, 1999, **186**, 222.
44 J. Novakova, L. Kubelkova and P. Jiru, *J. Chem. Soc., Faraday Trans.*, 1981, **77**, 1331.

Paper 9/06550D